

Numerical Modeling of Nitinol Stent Oversizing in Arteries with Clinically Relevant Levels of Peripheral Arterial Disease: The Influence of Plaque Type on the Outcomes of Endovascular Therapy

Can Gökgöl, MSc¹; Nicolas Diehm, MD, MBA^{2,3}; and Philippe Büchler, AP¹

¹Institute for Surgical Technology & Biomechanics, University of Bern, Switzerland.

²Clinical and Interventional Angiology, Vascular Institute Central Switzerland

³University of Applied Sciences Furtwangen, Villingen-Schwenningen, Germany

Nitinol Stent Oversizing in Peripheral Arteries with Calcified Plaques

Correspondence to:

Assoc. Prof. Dr. Philippe Büchler

Institute for Surgical Technology and Biomechanics

University of Bern

Stauffacherstrasse 78

Bern, CH-3014, Switzerland

Phone: +41 31 631 5947

Email: philippe.buechler@istb.unibe.ch

ABSTRACT

Oversizing of the Nitinol stents in the femoro-popliteal arterial tract is commonly performed by clinicians and further encouraged by stent manufacturers. However, in spite of the procedure's supposed benefits of strong wall apposition and increased luminal gain, its effects on the mechanical behavior of arteries with peripheral arterial disease are not fully clear. In this study, finite element analyses of endovascular revascularization of an idealized artery with 70% stenosis and three different plaque types have been performed to examine the influence of Nitinol stent oversizing on the arterial stresses and acute lumen gain. The analyses included the simulation of balloon angioplasty to model plaque failure, followed by stent implantation, in which four different oversizing ratios were investigated. Results showed that balloon angioplasty was crucial in determining the stress levels of the artery prior to stent implantation and heavily affected the outcome of endovascular therapy. For all plaque types, Nitinol stent oversizing was found to produce a marginal lumen gain in contrast to a significant increase in arterial stresses. For the arteries with lightly and moderately calcified plaques, oversizing was found to be non-critical; whereas for the arteries with heavily calcified plaques, the procedure should be avoided due to a risk of tissue failure.

Key words: Femoro-popliteal artery; calcification; finite element analysis (FEA); percutaneous transluminal angioplasty (PTA); plaque failure; stent deployment; stent mis-sizing; lumen gain; arterial stresses

Introduction

Endovascular treatment of Peripheral Arterial Disease (PAD) is ~~either~~ primarily performed by ~~either~~ percutaneous transluminal angioplasty (PTA) or through primary stent implantation following revascularization.^{18,33} In the case of the latter, choosing the correct stent size is crucial to simultaneously counteract arterial recoil and prevent extensive damage to the arterial tissues.^{38,47} However, due to a lack of established guidelines, the current clinical practice consists of the qualitative selection of the proper stent size based solely on recommendations provided by the stent manufacturers. As a result, Nitinol stent oversizing is frequently performed to maintain full wall apposition and prevent stent migration.^{25,36,38,47} Despite these perceived advantages, the large stresses inflicted onto the arteries due to oversizing might lead to arterial damage and, ultimately, to restenosis.^{8,20,37,45}

The number of studies on Nitinol stent oversizing in the peripheral vasculatory system are scarce. To date, there have only been two animal investigations that have studied the implications of coated and non-coated Nitinol stent oversizing in Yucatan swine and mini-pigs.^{38,47} Both studies have defined over-sized arteries as having a stent-to-artery ratio, i.e. the ratio of nominal stent diameter to lumen diameter of the artery, above 1.4 and suggested that while all the arteries have shown neointimal proliferation, only the oversized arteries (stent-to-artery ratio > 1.4) were damaged enough to exhibit restenosis. However, these studies were performed in healthy arteries and, as such, the results might not be applicable to the patient population that undergoes endovascular therapy of the lower limbs. A clinical study on stenosed carotid arteries supports this hypothesis, as the results suggest that oversized arteries (stent-to-artery ratio between 1.4 and 2.0) yield better outcomes in terms of late lumen loss compared to normal-sized arteries (stent-to-artery

ratio below 1.4).³⁶ These contradictory outcomes can be attributed not only to the differences in the vasculature systems, but also to the different morphologies and mechanics between healthy and diseased arterial layers. Therefore, to understand the effects of Nitinol stent oversizing on the actual clinical practice, the procedure should be evaluated on peripheral arteries with PAD.

Numerical analyses are routinely used to support or replace experiments with the intention to analyze the fatigue life of stents.^{15,29,30,34} They are also frequently used to understand the mechanical and hemodynamic behaviors of both healthy and diseased arteries due to stent implantation.^{3,8,17,24} In this instance, the numerical approach is a suitable substitute to performing clinical investigations that would be ethically questionable due to a high risk of damage to both the plaque and healthy arterial tissues. The majority of the previous numerical studies on stent mis-sizing have focused on balloon-expandable stents in coronary arteries.^{4,5,23,26} These studies have shown that stent implantation tends to disrupt the natural flow patterns and that oversizing (stent-to-artery ratio > 1.0) negatively impacts the Wall Shear Stress (WSS) and, consequently, increases the risk of restenosis. However, the results are not directly adaptable either to the endovascular procedures performed in lower-limbs or to the common clinical practice due to the differences in stent types, their deployment techniques and the use of healthy arterial models. On the other hand, the limited number of studies that cover Nitinol stent oversizing in peripheral arteries performed the analyses on non-calcified arteries.¹⁷ As such, the effects of Nitinol stent oversizing on the mechanical behavior of arteries with calcified plaques are currently not known. Therefore, the main aim of this study was to investigate the changes in arterial stresses and acute lumen gains associated with gradual stent oversizing. The numerical investigation was performed using finite element (FE) analyses of endovascular therapy in an artery model

that included clinically relevant PAD. A secondary objective was to observe whether the effects of oversizing were influenced by the degree of lesion calcification.

Materials and Methods

Components of the FE Simulations

Five parts were required for the FE modeling of the endovascular therapy; the diseased artery, the angioplasty balloon/s, the Nitinol stent, and the expansion and crimp tools. The artery was idealized as a straight cylinder with completely healthy sections at both ends and a mix of healthy and atherosclerotic tissue at the center for a total length of 35 mm (Fig. 1). Each healthy section had a length and lumen diameter of 5.0 mm⁴⁴ and were made of 3 layers²⁴; intima, media and adventita with thicknesses of 0.15 mm, 0.25 mm and 0.1 mm, respectively.^{40,41} The diseased section was created by increasing the thickness of the intimal layer to reach a luminal diameter that corresponded to 30% of the healthy lumen, ~~which is indicative of a clinically relevant PAD.~~ Since a 50% obstruction in the lumen diameter of a peripheral artery is considered as stenosis or in-stent restenosis and a 100% blockage is defined as a total case of occlusion^{1,46}, the 70% obstruction chosen for this study is between these two extremes and indicative of a clinically relevant PAD. By modifying the mechanical tissue properties of the thickened intimal layer to represent an atherosclerotic plaque, the stenosed tissue had been directly embedded into the artery. This approach enabled a geometrically smooth transition between the healthy and diseased sections and the resultant configuration corresponded to a symmetric plaque (Fig. 1a). ~~As it was previously shown that femoral plaques are typically heavily calcified^{10,12,14,19,27}, the plaque only included calcification and not any underlying sections of lipid pool or fibrotic tissues.~~ The plaque was modeled as a single geometrical entity; as such, the fibrotic tissue, the lipid pool and the calcification were not modeled separately. Instead, the plaque represented a mixture of calcified and non-calcified tissues through its mechanical properties. Each layer, including

the plaque, was discretized with linear hexahedral reduced integration elements (C3D8R). In each healthy section, the number of elements in intima, media and adventitia were approximately 4,000, 7,000 and 4,000, respectively. For the diseased section, the number of elements in the medial and adventitial layers were increased by approximately 2 times their healthy counterparts, while the plaque was meshed with approximately 50,000 elements. A mesh sensitivity analysis was performed to verify that the mesh was sufficiently dense to satisfy the convergence criteria defined in a previous study.¹⁷

The initial geometry of the angioplasty balloon corresponded to its fully-expanded configuration with a diameter of 5.0 mm and a length of 25 mm (Fig. 1b). The balloon had 4,000 linear quadrilateral membrane elements with reduced integration (M3D4R). A commercially available Nitinol stent, Astron-Pulsar (Biotronik AG, Bülach, Switzerland), with production dimensions of 80 μ m strut width, 155 μ m strut thickness, 3.5 mm outer diameter and 25 mm length was considered for the simulations (Fig. 1d). These dimensions represented the configuration right after the stent was laser-cut from a Nitinol tube and before the in-silico expansion and annealing. The number and type of elements for the stent were previously verified and corresponded to 170,000 linear reduced integration elements (C3D8R).¹⁷ The rigid expansion and crimp tools, which were used for the preconditioning and deployment of the stent, were both meshed with linear quadrilateral shell elements with reduced integration (S4R). The expansion tool had the same initial diameter as the inner diameter of the stent. Conversely, the diameter of the crimp tool corresponded to the unconstrained stent diameter achieved at the end of the preconditioning state and, as such, varied with each oversizing case (Fig. 1d).

Constitutive Models

The healthy arterial layers were represented with the Holzapfel-Gasser-Ogden (HGO) model; an anisotropic, hyper-elastic material model that includes two collagen fibre families.^{16,21} The material parameters were obtained from uniaxial tensile tests performed on the healthy portions of a single diseased external iliac artery acquired from autopsy. The exact values, including the fibre orientations and fibre dispersions within each layer, have been reported previously.^{17,21}

The atherosclerotic tissue was modeled as isotropic, hyper-elastic using a 3rd order reduced polynomial form (Yeoh) based on the ~~uniaxial~~ ~~planar tension experiments~~ ~~experimental data~~ performed on 20 samples of human atherosclerotic femoral plaques (Table 1).¹¹ The fitting was performed in Abaqus v.6.12 (Dassault Systemes, Simulia Corp., RI, USA) by providing the experimental data as the input for the material model. ~~It was previously shown that femoral plaques are typically heavily calcified.~~^{10,12,14,19,27} However, in order to cover the entirety of ~~the experimental data~~, three plaque groups (lightly calcified, moderately calcified and heavily calcified) were considered for the analyses. The ~~experiments~~ ~~experimental data~~ showed that the lightly calcified plaque underwent high stretch until tissue failure (0.3 MPa at a nominal strain of 1.15); while the moderately calcified plaque reached a higher ultimate tensile stress (0.43 MPa) at a nominal strain of 0.75. This ~~suggests~~ ~~shows~~ that the moderately calcified plaque was stiffer compared to the lightly calcified plaque. On the other hand, both the ultimate tensile stress and stretch values for the heavily calcified plaque were lower than the other plaque types (0.16 Mpa at a nominal strain of 0.55). ~~This behavior has been associated with the unique morphology of the heavily calcified plaque, which differs not only from the other femoral plaques, but also from the heavily calcified plaques from~~

~~other anatomical regions.³² However, as~~ As a result of its low failure stress and strain, the elastic mechanical response of the heavily calcified plaque prior to failure was very similar to the lightly calcified plaque.

Similar to previous studies that modeled plaque failure during endovascular therapy, a perfect plasticity model was adopted to represent tissue damage.^{6,8,9,15,35} This method allows the plaque to undergo plastic deformation, while preventing an increase in its stresses. Once the plastic limit is reached, the loads exerted onto the artery are transferred to the healthy layers. Upon unloading, the plaque is plastically deformed and the lumen diameter is permanently increased. At that point, the stresses in the healthy layers are determined by the extent of plastic deformation in the atherosclerotic tissues. The plasticity thresholds in this current study corresponded to the failure stress levels of each plaque group (Fig. 2).^{11,13} A justification for using failure stresses as yield stresses in the perfect plasticity model is provided in the discussion.

The angioplasty balloon was modeled with a linear, elastic material model. The material parameters, as well as a mass proportional Rayleigh damping coefficient, which was assigned to make the folding and inflation of the balloon more stable, were taken from literature.⁸ The material parameters for the super-elastic Nitinol model were provided by the manufacturer.¹⁷ Finally, the rigid crimp and expansion tools were represented with a linear, elastic model (Young's modulus E : 210,000 MPa; Poisson's ratio ν : 0.3).

Simulations of the Endovascular Therapy

The simulations were performed using Abaqus/Explicit with a user-defined, semi-automatic stable time increment of 4×10^{-6} . This value ensured that the kinetic energies of each individual part and the whole assembly remained below 5% of their corresponding internal

energies at any given time during the analyses. As a result, the quasi-static nature of the analyses was preserved at all time points of the simulations. A symmetry boundary condition was defined at the middle of the angioplasty balloon to prevent it from moving axially during the folding/unfolding steps. Finally, the artery was constrained at both ends to prevent movement in the longitudinal axis. A hard, frictionless contact was defined for the interactions between the balloon and the artery, as well as between the stent and the artery, using the general contact algorithm. On the other hand, the interactions between the tools and the stent were established with a surface-to-surface contact methodology, which ensured a proper separation of the surfaces.

Prior to the main analysis of endovascular therapy and stent oversizing, the initial configurations of the stent, the balloon and the artery were prepared through three standalone simulations. The first one was stent preconditioning, which consisted of an initial expansion of the stent to its unconstrained, i.e. nominal, diameter, followed by an annealing procedure that was performed to remove the stresses and preserve the expanded shape. A total of four oversizing ratios, 1.0, 1.2, 1.4, and 1.8, were investigated in this study. The unconstrained stent diameter for each case was calculated by multiplying these ratios with the healthy lumen diameter (i.e. 5 mm, 6 mm, 7 mm and 9 mm). For this simulation, the contact interaction between the outer surface of the expansion tool and the inner surface of the stent was activated. Subsequently, the stent was expanded by applying velocity boundary conditions to the nodes of the expansion tool. The second simulation was the folding of the angioplasty balloon by applying a negative pressure to the balloon's inner surface. The third and final simulation was an iterative process to determine the stress-free diameter of the artery, such that the healthy lumen diameter corresponded to the average diameter of the popliteal artery (i.e. 5 mm) under the physiological blood pressure of 120

mmHg.⁴² The deformed, stress-free configurations of the stent, the balloon and the artery were, then, brought together in a new assembly for the main analysis. In addition to these preparation simulations, the changes in the radial force profile of the stent with respect to different oversizing ratios were evaluated through further analyses, where the stents were crimped to their insertion diameter of 1.2 mm and expanded back to their unconstrained diameters.

The main analysis included the clinical processes of balloon angioplasty and stent implantation (Fig. 1). In the first step, the artery was pressurized by applying the physiological blood pressure of 120 mmHg on the inner surface of the artery (Fig. 1a). Next, the contact pair of balloon-artery was activated, and balloon angioplasty was simulated by applying a positive pressure of 7 atm. to the inner surface of the balloon (Fig. 1b). Subsequently, the balloon was folded and the minimum lumen diameter was checked to evaluate the success of the angioplasty (Fig. 1c). If the lumen diameter was below 70% of the healthy lumen diameter,¹⁵ then an additional angioplasty was performed using a larger balloon-diameter. Following the adequate expansion of the lumen, the contact interaction between the inner surface of the crimp tool and the outer surface of the stent was activated and the stent was crimped to its insertion diameter of 1.2 mm by radially displacing each node of the crimp tool (Fig. 1e). Finally, the contact pair of stent-artery was activated and the stent was expanded by radially expanding the crimp tool to its original position. As the stent came into contact with the artery, it detached from the crimp tool and was deployed into the artery (Fig. 1f).

Data Analysis

The effects of Nitinol stent oversizing were evaluated by analyzing the stress distribution (in particular, the 95th percentile) along the circumferential direction in the healthy layers surrounding the diseased region and the minimum lumen diameter at the end of pressurization, after balloon angioplasty and post stent deployment.

It is hypothesized that high arterial stresses possibly lead to adverse outcomes in patients.^{17,45} Since a stress threshold that puts the artery at risk is unknown, previous studies have investigated the effects of stent implantation based on tissue failure^{8,9}, which could be corroborated by experimental findings. Similarly, in this study, the 95th percentile stresses calculated with the numerical model were compared to the ultimate experimental stresses in the circumferential directions for the healthy layers surrounding the atherosclerotic tissue.¹⁶ The arterial layer identified as the most failure-prone was analyzed to establish the effects of endovascular therapy and Nitinol stent oversizing.

For the calculation of the minimum lumen diameter, the position of each node at the arterial lumen interface was extracted from Abaqus and exported to Matlab. Along the length of the artery, circles were fitted to each of the 108 rings of nodes representing the arterial lumen. The diameters of the circles corresponded to the lumen diameters along the length of the artery and the smallest one was reported as the minimum lumen diameter.

Additionally, the equivalent plastic strain (PEEQ) distributions, [as well as the 95th percentile PEEQ values at the integration points](#), in the atherosclerotic ~~tissue~~ tissues were reported to quantify plaque failure among the 3 different plaque types.

Results

The complete radial force profile of the stent clearly showed the super-elastic behavior of the Nitinol material,⁴³ where the stent's outward force remained near-constant across a wide range of diameters during crimping and deployment into the artery (Fig. 3). Increasing the oversizing ratio resulted in a higher radial force to be applied by the stent onto the artery during deployment. This difference was highest between the unconstrained stent diameters of 5 and 6 mm, which exhibited a 40% increase in the stent's radial force. The difference in the radial force was smaller – approx. 20% - when the unconstrained stent diameter increased from 7 to 9 mm. In contrast, the change in stent's radial force ~~is~~ was nominal (approx. 5%) between the unconstrained stent diameters of 6 and 7 mm.

Under the physiological blood pressure of 120 mmHg, the circumferential stresses in the healthy layers surrounding the diseased region, as well as the minimum lumen diameters, were comparable between the different plaque groups (Table 2). This suggested that all the artery models were in a similar mechanical condition prior to balloon angioplasty. The initial PTA with a 5 mm angioplasty balloon yielded different outcomes for the three plaque types. The minimum lumen diameters for the vessels with lightly, moderately and heavily calcified plaques were 2.5 mm, 3.2 mm and 3.4 mm, respectively (Table 3). At this stage, only the vessel with heavily calcified plaque satisfied the requirement to continue with stent implantation, as it was the only arterial model that reached a diseased lumen diameter corresponding to 70% of the healthy lumen diameter.¹⁵ This can be explained by the low stress-strain threshold (0.16 MPa at a nominal strain of 0.55) required to start the plastic deformation process in the heavily calcified plaque. As a result, the heavily calcified plaque underwent greater plastic deformation than both the moderately and lightly calcified

plaques, which reached their constant stress thresholds at considerably higher strain values of 0.75 and 1.15, respectively (Fig. 2).

To satisfy the deployment criteria, the arteries with lightly and moderately calcified plaques underwent a second PTA. The additional PTA of the artery with moderately calcified plaque using a 5.5 mm balloon yielded a lumen diameter of 3.5 mm. On the other hand, even with a 6 mm balloon, only a 3.0 mm lumen diameter could be reached for the artery with lightly calcified plaque, resulting in a partially successful balloon angioplasty. This can be attributed to the high amounts of stretch required to plastically deform the lightly calcified plaque. The PEEQ distributions in the atherosclerotic tissues following PTA support these observations (Fig. 4). Among the different plaque types, the heavily calcified plaque had the highest plastic strain not only at the lumen interface, but also along the thickness of the plaque after the initial balloon angioplasty (Fig. 4c). In line with the achieved lumen ~~gains~~ diameters, the lightly calcified plaque exhibited the least amount of plastic strain within the complete atherosclerotic tissue (Fig. 4a), while the plastic strain in the moderately calcified plaque ~~were~~ was in between the two groups (Fig. 4b). The 95th percentile PEEQ strain values after the 1st PTA for the lightly, moderately and heavily calcified plaques were 1.02, 1.33 and 1.42, respectively. A 2nd PTA significantly affected the plastic strain distribution in the moderately calcified plaque. The procedure increased the overall plastic strain level (the 95th percentile PEEQ strain = 1.41) and led to an increase in the volume that underwent plastic deformation (Fig. 4e). The final state slightly exceeded the distribution observed in the heavily calcified plaque after one PTA (Fig. 4c). Performing a 2nd PTA also had a similar effect on the distribution of plastic strain in the lightly calcified plaque (Fig. 4d). However, the overall plastic strain was still lower than the other plaque groups (the 95th percentile PEEQ strain = 1.33).

Following PTA, the arteries with heavily and moderately calcified plaques were in high stress states (Table 2). Additionally, they had similar stress values in the healthy layers surrounding the plaque. These can be attributed to the high levels of plastic strain observed in both plaque types. Comparatively, the stresses in the artery with lightly calcified plaque were significantly lower as its atherosclerotic tissue underwent a smaller plastic deformation than the other plaque types.

The implantation of a Nitinol stent further increased the stresses and lumen diameters in all the artery models (Tables 2 & 3). However, compared to PTA, the procedure did not cause any additional plastic deformation. As a result, the outcome of the stenting procedure is directly influenced by the hyperelastic behavior, i.e. the mechanical stiffness, of the plaque, since the plaque tissue continued to support the loads exerted onto the artery following PTA.

Regardless of the oversizing ratio and the plaque type, the 95th percentile circumferential stresses in the media following Nitinol stent implantation was found to be approximately 60 kPa. As such, the stresses in the medial layer only reached up to 15% of the tissue's ultimate tensile stress of 420 kPa.¹⁶ In comparison, even in the model with the lowest stresses in the adventitia, the values reached up to 30% of the failure stress of 1,300 kPa. Based on ~~the stress levels~~ this observation, the most failure-prone healthy layer was found to be the adventitia. Figure 5 shows the stress distribution of the artery with moderately calcified plaque following Nitinol stent implantation with different oversizing ratios. Regardless of the oversizing ratio, the artery with heavily calcified plaque always had the highest circumferential stresses and lumen diameter (Fig. 6). This can be attributed to the high stress-state of the artery following PTA and the low stiffness of the plaque (Fig. 2). On the

other hand, while the lightly calcified plaque had a similar stiffness as the heavily calcified plaque, the artery always had the lowest circumferential stresses and lumen diameter. This low level of stress directly results from the low stress-state following balloon angioplasty.

Stent implantation has led to a narrow distribution of the stresses in the arteries with lightly and ~~moderately~~ heavily calcified plaques (Fig. 6). Again, this can be attributed to the low stiffness of the plaque tissues, allowing a uniform deformation and stress increase along the entire tissue. In contrast, the stress distribution in the artery with moderately calcified plaques was much wider, with lower minimum values than the stress levels observed in the arteries with lightly calcified plaques. This can be explained by the higher stiffness of the moderate plaque, acting as a stronger barrier that limits the amount of load transferred to the healthy tissues.

For all plaque groups, increasing the oversizing ratio led to a linear increase in the circumferential stresses (Fig. 7). Similarly, a linear relationship was observed between the oversizing ratio and the lumen diameter (Fig. 7). The artery with heavily calcified plaque, followed by the artery with lightly calcified plaque, exhibited the largest increase in arterial stresses with increased oversizing. Correspondingly, these two plaque types had the largest increases in the acute lumen gains with oversizing. The similar behavior between these two arterial models can be attributed to the similar stiffness of the lightly and heavily calcified plaques (Fig. 2). In comparison, the artery with moderately calcified plaque was the least affected in terms of arterial stresses and lumen gain due to the high stiffness of its plaque.

Discussion

Nitinol stent oversizing is a term used to describe the ratio and, in extreme cases, the mismatch between healthy lumen and stent diameters.^{38,47} The procedure can occur either on purpose, by selecting a stent diameter that is larger than the healthy lumen diameter, or inadvertently, by implanting a single long stent over a considerably long lesion (>300 mm), which results in a mismatch between the constant stent diameter and the narrowing lumen.^{7,25} Currently, stent manufacturers provide a stent-specific value as the recommended oversizing ratio. However, the bases for selecting these values are unclear. With no objective guidelines, clinicians either avoid oversizing and, as a result, do not utilize the procedure's possible advantages (i.e. preventing stent migration, achieving a desirable lumen gain immediately after implantation etc.),³⁶ or they tend to oversize the stents and risk arterial damage. More recently, animal studies and numerical analyses have been conducted to define an ideal oversizing ratio for the peripheral arteries.^{38,47} However, they were limited by the use of healthy arteries, whose morphologies are considerably different than diseased arteries. Thus, to understand the real-world implications of Nitinol stent oversizing, these studies should primarily be conducted on diseased arteries. Therefore, the aim of this study was to investigate the effects of Nitinol stent oversizing on the mechanical behavior of peripheral arteries by performing in-silico analyses of endovascular therapy in arterial models with a clinically relevant model of PAD. Furthermore, three different plaque types were considered in the model to evaluate whether the severity of plaque calcification has any influence on the treatment outcomes.

The mechanical behavior of the artery during PTA is strongly affected by the plaque type. [At this point of the procedure, the stiffness of the plaque had little influence on the final](#)

configurations of the dilated arteries. Instead, both the arterial stresses and lumen gain were directly defined by the strain values that corresponded to the start of plastic deformation in the plaque tissues (Table 1).¹³ Between the lightly and moderately calcified plaques, the former had to undergo a comparatively higher stretch to reach its plastic limit (Fig. 2). On the other hand, the stress and strain values associated with the plasticity threshold of the heavily calcified artery was considerably lower than the other plaque types. ~~These strain values (Table 1)¹³ directly defined the configurations of the arteries following PTA.~~ Thus, two of the artery types required a 2nd balloon angioplasty to achieve a satisfactory lumen diameter due to the high stretching ~~that was~~ necessary to start plastic deformation in their plaques. A 2nd PTA increased the amount of plastic strain in the moderately calcified plaque (Fig. 4d) to similar levels observed in the heavily calcified plaque after one PTA (Fig. 4c). This meant that both plaque types experienced similar amounts of plastic deformation, which can also be inferred from the similar lumen diameters and arterial stresses between the two artery types (Tables 2 & 3). For the lightly calcified artery, even a second PTA was insufficient to reach the level of strain needed to undergo the same level of plastic deformation as the other plaque types. As a result, the arteries with moderately and heavily calcified plaques were both in a higher stress state compared to the artery with lightly calcified plaque following PTA.

The type of plaque also affected the outcomes following Nitinol stent implantation. ~~In contrast to the mechanism behind the final configuration of the arteries following PTA, the effects of Nitinol stent implantation were not determined by the plastic stress or strain thresholds. Due to the use of perfect plasticity as a damage model~~ Since damage was modeled as perfect plasticity, the deformed plaque continued to support the loads exerted onto the artery by the stent. However, unlike the situation during PTA, only the hyper-elastic

behavior of the plaque ~~influenced~~ **determined** the final configuration of the artery, as no additional plastic deformation was observed during stent deployment. As a result, the lumen gain obtained following stent implantation was considerably lower than the ~~one~~ **gain** achieved after PTA. **At this point of the procedure, the differences and similarities in both the stress states and lumen gain between the different plaque types directly resulted from the stiffness of the plaques.** The artery with heavily calcified plaque had a substantial increase in adventitial stresses following stent implantation due to its low mechanical stiffness in the elastic region (Table 2). Although being at a comparatively lower stress state after PTA, the artery with lightly calcified plaque also had a significant increase, which can be attributed to the similar mechanical stiffness of the two plaque types (Fig. 2). On the other hand, the artery with moderately calcified plaque had the least increase in adventitial stresses with stent implantation due to the higher stiffness of the moderate plaque. **In that sense, the presence of a moderately calcified plaque would decrease the risk of arterial damage by limiting the stress increase in the healthy arterial layers.** These outcomes were accordingly reflected in the lumen ~~gain~~ **diameters** observed following stent deployment, with the arteries with heavily and lightly calcified plaques achieving a similar and higher lumen gain compared to the artery with moderately calcified plaque (Table 3) (Fig. 7).

For all plaque types, the increases in adventitial stresses and acute lumen ~~gains~~ with respect to Nitinol stent oversizing were heavily dependent on the stent's radial force profiles for different oversizing ratios (Fig. 3). A larger increase in the radial force of the stent has led to a correspondingly large increase in both arterial stresses and lumen diameters. As such, increasing the oversizing ratio from 1.0 to 1.2 (5 mm to 6 mm) or from 1.4 to 1.8 (7 mm to 9 mm) had a bigger effect on the mechanical response of the artery compared to the similar outcomes obtained with increasing the ratio from 1.2 to 1.4 (6 mm to 7 mm) (Tables 2 & 3).

Despite this, the relationship between the arterial stresses (the 95th percentile, the 75th percentile and the median values) and the oversizing ratio, as well as the relation between the acute lumen gains and the unconstrained stent diameters, was found to be well approximated with a linear function for all plaque groups (Figs. 6 & 7). However, a mismatch between the increases in arterial stresses and lumen gain was also present with oversizing (i.e. 31% stress increase vs. 4% increase in the lumen gain when the oversizing ratio was increased from 1.0 to 1.8 for the artery with lightly calcified plaque).

Comparison of the results with an oversizing study conducted in healthy peripheral arteries showed that the outcomes of the procedure differed significantly between the two artery types.¹⁷ Oversizing of healthy arteries led to nonlinear increases in both arterial stresses and lumen gains (Fig. 7). Furthermore, regardless of the plaque type, diseased arteries were less sensitive to oversizing, showcased by a smaller increase in adventitial stresses between each oversizing ratio. This can be explained by the difference in the distribution of the loads between the healthy and diseased arteries. Whereas the adventitia primarily supported the majority of the mechanical load in the healthy artery, in the diseased arteries, the load was distributed between the plastically deformed plaque and the adventitia. [This suggests that the plaque tissue acts as a protective layer between the stent and the healthy layers by preventing a critical increase in arterial stresses.](#)

Following stent implantation, the arteries with moderately and heavily calcified plaques exhibited higher stresses compared to the healthy artery. This result can be attributed to the revascularization of the artery with PTA. This procedure was only performed in the diseased arteries and determined the arterial stresses prior to stent deployment. By comparison, the stress levels in the arteries with moderately and heavily ~~calcified~~ calcified plaques after PTA

corresponded to the stresses calculated in the healthy artery with an oversized stent of 5.5 mm. At this stage, deploying a stent in the arteries with moderately and heavily calcified plaques further increased their high stress levels and ensured that their final stress states would be higher than the healthy artery. On the other hand, the artery with lightly calcified plaque was at a low stress state after PTA and the additional stresses produced by stents did not exceed the stress levels in the healthy arteries.

In terms of lumen gain, ~~the results~~ previous numerical and experimental studies suggested that the adventitia ~~acted~~ acts as a protective layer and ~~prevented~~ prevents the artery from significant expansion in healthy arteries.^{16,17,22} In the diseased arteries, however, the stent continued to push against the plaque, without producing any additional plastic deformation. As such, the resultant lumen gain was determined by the stiffness of the plaque tissue. Since the arteries with lightly and heavily calcified arteries had a low mechanical stiffness, they produced a higher lumen gains than the non-calcified arteries. Despite these differences, the mismatch between the low lumen gain induced by stent oversizing and the large increase of the arterial stresses was also observed for the healthy arteries.

Several assumptions had to be made within the current numerical framework. Within the diseased region, the intimal layer was replaced with the plaque tissue. However, since the adventitia becomes the mechanically predominant layer under high pressures (following PTA),^{22,31,39} the influence of the intimal layer on the mechanical behavior of the artery would be small and can be neglected. The artery was not pre-stressed, which may decrease the final values of the stresses observed after stent implantation. However, arterial pre-stressing would not affect the linear relation between the oversizing ratio and either the stresses or the lumen gain.

Concerning the experimental data adopted for this study, it should be noted that the mechanical behavior of the heavily calcified plaque seems counter-intuitive. Its failure stress and strain are lower than the other plaque types and its stiffness is very similar to the lightly calcified plaque. The authors of the data explained that this behavior is associated with this plaque's unique morphology, which is different from other plaque types.¹¹ Further explanations can be derived from a recent experimental study performed on the carotid plaque tissues, which exhibited a similar mechanical behavior as the femoral plaques.² Through ex-vivo computer tomography (CT) imaging, the carotid samples were characterized as a mixture of calcified and non-calcified tissues. The calcification was suggested to act as a mechanical restraint to the applied loading. As such, the plaque deformation was only restricted to the stretching of the non-calcified tissue. This explains the reduced failure stretch with increasing calcification, as the remaining tissue available for stretching is decreased. On the other hand, the increased plaque strength has been postulated to be caused by a strong adhesion between the calcified and non-calcified tissues that compose the samples. Although this recent study brings new insights to the experimental data used in the current numerical models, additional experiments on the femoral tissues are needed to confirm these observations.

The model of perfect plasticity that is used for reconfiguring the plaque tissue represents a simplified approach to the failure of the calcified plaque. Although not exactly a failure model, perfect plasticity is commonly used to model plaque failure during endovascular therapy.^{6,8,9,15,35} The majority of these studies have set the stress threshold at 400 kPa^{6,8,9}, which corresponded to an average value of plaque failure under uniaxial tensile tests.²⁸ The remaining studies have used 270 kPa, which represented the rupture stress of a single atherosclerotic plaque.^{15,35} Conway et al. have justified using the ultimate tensile stresses as

the plastic stress threshold by conducting a parametric study with different values.⁹ Their results showed that the variances in the stress threshold had a marginal effect on the mechanical behavior of the artery; changing the yield stress from 200 kPa to 400 kPa resulted in less than a 5% change in vessel recoil for all plaque types. Recently, Chiastra et al. have used the same methodology to simulate PTA and stent implantation in numerical models of coronary bifurcation.⁶ A combination of CT angiography and Optical Coherence Tomography (OCT) was used to validate the simulations. The results showed approximately 15%-20% error between the calculated shape of the artery and the experimental reconstruction based on the Hybrid OC-CT methodology. The results from both of these studies suggested that using failure stresses as a plastic threshold is a suitable approximation to model plaque failure.

In any case, there is no information in the literature that suggests the plaque actually behaves the way it is modeled in this study during balloon angioplasty. Furthermore, with this model, the deformed plaque continues to support the loads that are exerted onto the artery by the stent, which may lead to an underestimation of the arterial stresses. Experimental and clinical studies that focus on understanding the failure behavior of the plaque should be undertaken to improve the existing knowledge and modeling of the failure characteristics of the atherosclerotic tissues. Finally, the results provide an overview of Nitinol stent oversizing based on a single stent design. Although we believe that the general behavior would be similar for other designs, the actual stress values and lumen diameters would likely be different.

Conclusion

Despite Nitinol stent oversizing being routinely performed during endovascular interventions, the number of experimental and numerical studies that investigate the effects of the procedure has been limited. Furthermore, the studies have been performed almost exclusively on healthy arterial models and completely overlooked the plaque tissue, the procedure of balloon angioplasty and the effect of the reconfigured calcified plaque on the outcomes of stent deployment. Therefore, this study used arterial models with calcified plaques in order to give some insights on the implications of Nitinol stent oversizing in patients undergoing endovascular revascularizations. PTA was the primary force behind achieving a substantial lumen gain and the procedure significantly contributed to the final stress state of the artery. As Nitinol stent implantation did not cause any additional plastic deformation, the mechanical stiffness of the plaques determined the additional lumen gain and arterial stresses produced following stent deployment. [Compared to the healthy arteries, the plaque tissues present in the diseased arteries acted as a protective barrier during stent implantation by limiting the amount of stresses transmitted to the healthy arterial layers.](#) Among the different plaque types, oversizing seems not to be critical for the arteries with lightly and moderately calcified plaques; the former being at a lower stress state after PTA (due to the high strain level required to induce plastic deformations) and the latter having the least increase in adventitial stresses with oversizing (due to the stiff plaque behavior). However, for both cases, the procedure only produced a marginal lumen gain. For the arteries with heavily calcified plaques, oversizing should be avoided as the low stiffness of the plaque led to an increase of an already high stress state achieved following PTA (due to the low plasticity threshold) towards the failure limit of adventitia.²¹ These results further

support the notion that Nitinol stents are inherently made to act as scaffolds and not as instruments to facilitate additional lumen expansion.

Acknowledgements

This investigation was supported by the Research Council of the Kantonsspital Aarau, the Swiss Heart Foundation and the Gotthard Schettler Foundation. The authors have no commercial, proprietary, or financial interest in any products or companies described in this article.

References

1. Alfonso, F., R. a. Byrne, F. Rivero, and A. Kastrati. Current treatment of in-stent restenosis. *J. Am. Coll. Cardiol.* 63:2659–2673, 2014.
2. Barrett, H. E., E. M. Cunnane, E. G. Kavanagh, and M. T. Walsh. On the effect of calcification volume and configuration on the mechanical behaviour of carotid plaque tissue. *J. Mech. Behav. Biomed. Mater.* 56:45–56, 2016.
3. Boland, E. L., J. a. Grogan, C. Conway, and P. E. McHugh. Computer Simulation of the Mechanical Behaviour of Implanted Biodegradable Stents in a Remodelling Artery. *Jom* 68:1198–1203, 2016.
4. Chen, H. Y., B.-K. Koo, D. L. Bhatt, and G. S. Kassab. Impact of stent mis-sizing and mis-positioning on coronary fluid wall shear and intramural stress. *J. Appl. Physiol.* 115:285–292, 2013.
5. Chen, H. Y., a. K. Sinha, J. S. Choy, H. Zheng, M. Sturek, B. Bigelow, D. L. Bhatt, and G. S. Kassab. Mis-sizing of stent promotes intimal hyperplasia: impact of endothelial shear and intramural stress. *AJP Hear. Circ. Physiol.* 301:H2254–H2263, 2011.
6. Chiastra, C., W. Wu, B. Dickerhoff, A. Aleiou, G. Dubini, H. Otake, F. Migliavacca, and J. F. LaDisa. Computational replication of the patient-specific stenting procedure for coronary artery bifurcations: From OCT and CT imaging to structural and hemodynamics analyses. *J. Biomech.* 49:2102–2111, 2015.
7. Cho, H., M. Nango, Y. Sakai, E. Sohgawa, K. Kageyama, S. Hamamoto, T. Kitayama, A. Yamamoto, and Y. Miki. Neointimal hyperplasia after stent placement across size-discrepant vessels in an animal study. *Jpn. J. Radiol.* 32:340–6, 2014.
8. Conway, C., J. P. McGarry, and P. E. McHugh. Modelling of Atherosclerotic Plaque for Use in a Computational Test-Bed for Stent Angioplasty. *Ann. Biomed. Eng.* 42:2425–2439, 2014.
9. Conway, C., F. Sharif, J. P. McGarry, and P. E. McHugh. A Computational Test-Bed to Assess Coronary Stent Implantation Mechanics Using a Population-Specific Approach. *Cardiovasc. Eng. Technol.* 3:374–387, 2012.
10. Cunnane, E. M., H. E. Barrett, E. G. Kavanagh, R. Mongrain, and M. T. Walsh. The influence of composition and location on the toughness of human atherosclerotic femoral plaque tissue. *Acta Biomater.* 31:264–275, 2016.
11. Cunnane, E. M., J. J. Mulvihill, H. E. Barrett, D. A. Healy, E. G. Kavanagh, S. R. Walsh, and M. T. Walsh. Mechanical, biological and structural characterization of human atherosclerotic femoral plaque tissue. *Acta Biomater.* 11:295–303, 2015.

12. Cunnane, E. M., J. J. E. Mulvihill, H. E. Barrett, M. M. Hennessy, E. G. Kavanagh, and M. T. Walsh. Mechanical properties and composition of carotid and femoral atherosclerotic plaques: A comparative study. *J. Biomech.* 49:3697–3704, 2016.
13. Cunnane, E. M., J. J. E. Mulvihill, H. E. Barrett, and M. T. Walsh. Simulation of human atherosclerotic femoral plaque tissue : the influence of plaque material model on numerical results. *Biomed. Eng. Online* 14:S7, 2015.
14. Derksen, W. J. M., J. P. P. M. De Vries, A. Vink, E. Velema, J. A. Vos, D. De Kleijn, F. L. Moll, and G. Pasterkamp. Histologic atherosclerotic plaque characteristics are associated with restenosis rates after endarterectomy of the common and superficial femoral arteries. *J. Vasc. Surg.* 52:592–599, 2010.
15. Dordoni, E., A. Meoli, W. Wu, G. Dubini, F. Migliavacca, G. Pennati, and L. Petrini. Fatigue behaviour of Nitinol peripheral stents: The role of plaque shape studied with computational structural analyses. *Med. Eng. Phys.* 36:842–849, 2014.
16. Gasser, T. C., R. W. Ogden, and G. a Holzapfel. Hyperelastic modelling of arterial layers with distributed collagen fibre orientations. *J. R. Soc. Interface* 3:15–35, 2006.
17. Gökgöl, C., N. Diehm, F. R. Nezami, and P. Büchler. Nitinol Stent Oversizing in Patients Undergoing Popliteal Artery Revascularization: A Finite Element Study. *Ann. Biomed. Eng.* 43:2868–2880, 2015.
18. Gornik, H. L., and J. a Beckman. Cardiology patient page. Peripheral arterial disease. *Circulation* 111:e169–72, 2005.
19. Herisson, F., M. F. Heymann, M. Chétiveaux, C. Charrier, S. Battaglia, P. Pilet, T. Rouillon, M. Krempf, P. Lemarchand, D. Heymann, and Y. Gouëffic. Carotid and femoral atherosclerotic plaques show different morphology. *Atherosclerosis* 216:348–354, 2011.
20. Hoffmann, R., G. S. Mintz, J. J. Popma, L. F. Satler, a D. Pichard, K. M. Kent, C. Walsh, P. Mackell, and M. B. Leon. Chronic arterial responses to stent implantation: a serial intravascular ultrasound analysis of Palmaz-Schatz stents in native coronary arteries. *J. Am. Coll. Cardiol.* 28:1134–9, 1996.
21. Holzapfel, G. a. Mechanics of Angioplasty: Wall, Balloon and Stent. *Casey J., Bao G. Mech. Biol. ASME* , 2000.
22. Holzapfel, G. A., G. Sommer, and P. Regitnig. Anisotropic mechanical properties of tissue components in human atherosclerotic plaques. *J. Biomech. Eng.* 126:657–65, 2004.
23. Holzapfel, G. A., M. Stadler, and T. C. Gasser. Changes in the mechanical environment of stenotic arteries during interaction with stents: computational assessment of parametric stent designs. *J. Biomech. Eng.* 127:166–80, 2005.

24. Holzapfel, G. a., M. Stadler, and C. a. J. Schulze-Bauer. A Layer-Specific Three-Dimensional Model for the Simulation of Balloon Angioplasty using Magnetic Resonance Imaging and Mechanical Testing. *Ann. Biomed. Eng.* 30:753–767, 2002.
25. Kirsch, E. C., M. S. Khangure, P. Morling, T. J. York, and W. Mcauliffe. Oversizing of Self-Expanding Stents : Influence on the Development of Neointimal Hyperplasia of the Carotid Artery in a Canine Model. 121–127, 2002.
26. LaDisa, J. F., L. E. Olson, I. Guler, D. a Hettrick, J. R. Kersten, D. C. Warltier, and P. S. Pagel. Circumferential vascular deformation after stent implantation alters wall shear stress evaluated with time-dependent 3D computational fluid dynamics models. *J. Appl. Physiol.* 98:947–57, 2005.
27. Li, F., M. M. McDermott, D. Li, T. J. Carroll, D. S. Hippe, C. M. Kramer, Z. Fan, X. Zhao, T. S. Hatsukami, B. Chu, J. Wang, and C. Yuan. The association of lesion eccentricity with plaque morphology and components in the superficial femoral artery: a high-spatial-resolution, multi-contrast weighted CMR study. *J. Cardiovasc. Magn. Reson.* 12:37, 2010.
28. Loree, H. M., A. J. Grodzinsky, S. Y. Park, L. J. Gibson, and R. T. Lee. Static circumferential tangential modulus of human atherosclerotic tissue. *J. Biomech.* 27:195–204, 1994.
29. Meoli, A., E. Dordoni, L. Petrini, F. Migliavacca, G. Dubini, and G. Pennati. Computational Modelling of In Vitro Set-Ups for Peripheral Self-Expanding Nitinol Stents: The Importance of Stent-Wall Interaction in the Assessment of the Fatigue Resistance. *Cardiovasc. Eng. Technol.* 4:474–484, 2013.
30. Migliavacca, F., L. Petrini, P. Massarotti, S. Schievano, F. Auricchio, and G. Dubini. Stainless and shape memory alloy coronary stents: a computational study on the interaction with the vascular wall. *Biomech. Model. Mechanobiol.* 2:205–17, 2004.
31. Moreno, P. R., K. R. Purushothaman, V. Fuster, and W. N. O'Connor. Intimomedial interface damage and adventitial inflammation is increased beneath disrupted atherosclerosis in the aorta: Implications for plaque vulnerability. *Circulation* 105:2504–2511, 2002.
32. Mulvihill, J. J., E. M. Cunnane, S. M. McHugh, E. G. Kavanagh, S. R. Walsh, and M. T. Walsh. Mechanical, biological and structural characterization of in vitro ruptured human carotid plaque tissue. *Acta Biomater.* 9:9027–35, 2013.
33. Norgren, L., W. R. Hiatt, J. a Dormandy, M. R. Nehler, K. a Harris, and F. G. R. Fowkes. Inter-Society Consensus for the Management of Peripheral Arterial Disease (TASC II). *J. Vasc. Surg.* 45 Suppl S:S5–67, 2007.
34. Petrini, L., A. Trotta, E. Dordoni, F. Migliavacca, G. Dubini, P. V. Lawford, J. N. Gosai, D. M. Ryan, D. Testi, and G. Pennati. A Computational Approach for the Prediction of

Fatigue Behaviour in Peripheral Stents: Application to a Clinical Case. *Ann. Biomed. Eng.* , 2015.doi:10.1007/s10439-015-1472-7

35. Petrini, L., W. Wu, E. Dordoni, A. Meoli, F. Migliavacca, and G. Pennati. Fatigue Behavior Characterization of Nitinol for Peripheral Stents. *Funct. Mater. Lett.* 05:1250012, 2012.
36. Piamsomboon, C., G. S. Roubin, M. W. Liu, S. S. Iyer, A. Mathur, L. S. Dean, C. R. Gomez, J. J. Vitek, N. Chattipakorn, and G. Yates. Relationship Between Oversizing of Self-Expanding Stents and Late Loss Index in Carotid Stenting. *Cathet. Cardiovasc. Diagn.* 143:139–143, 1998.
37. Rebelo, N., R. Fu, and M. Lawrenchuk. Study of a Nitinol Stent Deployed into Anatomically Accurate Artery Geometry and Subjected to Realistic Service Loading. *J. Mater. Eng. Perform.* 18:655–663, 2009.
38. Saguner, A. M., T. Traupe, L. Räber, N. Hess, Y. Banz, A. R. Saguner, N. Diehm, and O. M. Hess. Oversizing and restenosis with self-expanding stents in iliofemoral arteries. *Cardiovasc. Intervent. Radiol.* 35:906–13, 2012.
39. Schulze-bauer, C. A. J., P. Regitnig, and G. A. Holzapfel. Mechanics of the human femoral adventitia including the high-pressure response. *Am J Physiol Hear. Circ Physiol* 282:2427–2440, 2002.
40. Smilde, T. J., F. W. van den Berkmortel, G. H. Boers, H. Wollersheim, T. de Boo, H. van Langen, and a F. Stalenhoef. Carotid and femoral artery wall thickness and stiffness in patients at risk for cardiovascular disease, with special emphasis on hyperhomocysteinemia. *Arterioscler. Thromb. Vasc. Biol.* 18:1958–1963, 1998.
41. Stary, H. C., D. Blankenhorn, a B. Chandler, S. Glagov, W. Insull, M. Richardson, M. E. Rosenfeld, S. Schaffer, C. J. Schwartz, and W. D. Wagner. A Definition of the Intima of Human Arteries and of Its Atherosclerosis-Prone Regions. *Circulation* 85:391–405, 1992.
42. Stiegler, H., and R. Brandl. Importance of ultrasound for diagnosing peripheral arterial disease. *Ultraschall Med.* 30:334–74, 2009.
43. Stoeckel, D., A. Pelton, and T. Duerig. Self-expanding Nitinol stents: Material and design considerations. *Eur. Radiol.* 14:292–301, 2004.
44. Tai, N. R., a Giudiceandrea, H. J. Salacinski, a M. Seifalian, and G. Hamilton. In vivo femoropopliteal arterial wall compliance in subjects with and without lower limb vascular disease. *J. Vasc. Surg.* 30:936–45, 1999.
45. Timmins, L. H., M. W. Miller, F. J. Clubb, and J. E. Moore. Increased artery wall stress post-stenting leads to greater intimal thickening. *Lab. Invest.* 91:955–67, 2011.

46. Zeller, T. Current state of endovascular treatment of femoro-popliteal artery disease. *Vasc. Med.* 12:223–34, 2007.
47. Zhao, H. Q., A. Nikanorov, R. Virmani, R. Jones, E. Pacheco, and L. B. Schwartz. Late stent expansion and neointimal proliferation of oversized Nitinol stents in peripheral arteries. *Cardiovasc. Intervent. Radiol.* 32:720–6, 2009.

-	C10 (MPa)	C20 (MPa)	C30 (MPa)	Plasticity Threshold	
Calcification				Stress (MPa)	Strain
Light	$5.9 \cdot 10^{-2}$	$4.4 \cdot 10^{-3}$	$-2.7 \cdot 10^{-4}$	$3.0 \cdot 10^{-1}$	1.15
Moderate	$1.4 \cdot 10^{-1}$	$3.1 \cdot 10^{-2}$	$-1.6 \cdot 10^{-2}$	$4.3 \cdot 10^{-1}$	0.75
Heavy	$4.7 \cdot 10^{-2}$	$1.5 \cdot 10^{-2}$	$-1.3 \cdot 10^{-2}$	$1.2 \cdot 10^{-1}$	0.55

Table 1: Material parameters (C10, C20 and C30) of the Yeoh SEF model for the arteries with lightly, moderately and heavily calcified plaques represent the average mechanical behavior of the plaque tissue under ~~uniaxial-extension~~ planar tension tests^{11,13}. The plasticity threshold corresponds to the failure stress of the tissues.

	Circumferential Stresses (kPa) (95th Percentile)						
	Pre-Angio (@ 120 mmHg)	Post 1 st Balloon Angioplasty	Post 2 nd Balloon Angioplasty	Post Stent Implantation			
				Unconstrained Stent Diameter			
				5 mm	6 mm	7 mm	9 mm
Calcification							
Light	0.6	32	140	371	458	485	543
Moderate	0.1	161	356	559	590	600	641
Heavy	0.8	303	-	732	833	851	922

Table 2: The circumferential stresses (95th percentile) in the adventitial layer following the pressurization of the artery with a physiological blood pressure of 120 mmHg (Pre-Angio), balloon angioplasty and stent implantation for the arteries with lightly, moderately and heavily calcified plaques.

	Minimum Lumen Diameter (mm)						
	Pre-Angio (@ 120 mmHg)	Post 1 st Balloon Angioplasty	Post 2 nd Balloon Angioplasty	Post Stent Implantation			
				Unconstrained Stent Diameter			
				5 mm	6 mm	7 mm	9 mm
Calcification							
Light	1.46	2.51	2.98	3.45	3.50	3.51	3.57
Moderate	1.39	3.16	3.49	3.68	3.71	3.71	3.74
Heavy	1.48	3.44	-	3.83	3.89	3.90	3.95

Table 3: The minimum lumen diameter following the pressurization of the artery with a physiological blood pressure of 120 mmHg (Pre-Angio), balloon angioplasty and stent implantation for the arteries with lightly, moderately and heavily calcified plaques.

Figure Captions

Figure 1: The complete procedure of an endovascular therapy in an artery with a clinically relevant level of PAD (70% stenosis): The pressurization of the artery with the physiological blood pressure of 120 mmHg and the positioning of the angioplasty balloon (a), unfolding of the angioplasty balloon with a pressure of 7 atm to simulate plaque failure (b), folding of the angioplasty balloon and evaluation of the expanded lumen diameter (c), representation of the Nitinol stent and the crimp tool in their unconstrained diameters prior to crimping of the stent (d), crimping of the Nitinol stent to a crimp diameter of 1.2 mm to simulate insertion into the artery (e), and the deployment of the stent into the artery (f).

Figure 2: The average stress-strain behaviors of the lightly (n=3), moderately (n=5) and heavily (n=12) calcified femoral plaque types under ~~uniaxial tensile~~ ~~planar tension~~ tests show that the moderately calcified plaque have the highest stiffness; while the lightly and heavily calcified plaque types have similar mechanical behaviors prior to tissue failure.¹¹ The tissue damage was modeled using perfect plasticity with the heavily calcified plaque reaching its constant stress threshold the earliest (160 kPa at a nominal strain of 0.55) and the lightly calcified plaque reaching it the latest (300 kPa at a nominal strain of 1.15) (Table 1).

Figure 3: The radial force profiles of the Nitinol stent for each of the unconstrained stent diameters showed that increasing the oversizing ratio led to an increase in the radial force of the stent during crimping and deployment into the artery. As a result, the 9 mm stent exerted the highest radial force onto the artery, whereas the 5 mm stent exerted the lowest. On the other hand, the difference between the radial forces of the 6 and 7 mm stents during deployment was found to be marginal. For visualization purposes, the full radial force profile during the crimping and deployment of stent is only shown for the 9 mm stent.

Figure 4: The PEEQ distributions in the atherosclerotic tissues following the 1st PTA showed that the heavily calcified plaque had the largest plastic strain and, as such, the largest plastic deformation (c). The extent of plastic deformation was followed by the moderately calcified plaque (b) and, finally, the lightly calcified plaque (a). Performing a 2nd PTA resulted in a significant increase in the plastic strain level of the moderately calcified plaque (e). On the other hand, while the 2nd PTA also increased the extent of plastic deformation experienced by the lightly calcified plaque; the overall plastic strain was still lower than the other plaque types (d).

Figure 5: The stress distribution in the artery with moderately calcified plaque following stent implantation showed that, regardless of the oversizing ratio, the most failure-prone layer was the healthy adventitia over the diseased region. Increasing the oversizing ratio led to an increase in the circumferential stresses of the artery, with the 9 mm stent (d) producing the highest stress, followed by the 7 mm stent (c), the 6 mm stent (b) and, finally, the 5 mm stent (a).

Figure 6: The stress distribution in the healthy adventitia has been reported for the different plaque types and oversizing ratios. Similar to the 95th percentile, the average stresses were the lowest lower for the artery with the lightly calcified plaque, followed by and the highest for the arteries artery with moderately and heavily calcified plaques. The stress values in the adventitia showed a larger scattering for the artery with the moderately calcified plaque than for the other types of calcification. The wider distribution can be attributed to the plaque stiffness. Despite these differences, there was a linear relationship between the unconstrained stent diameters and the circumferential stresses (the 95th percentile, the 75th percentile, as well as the median values) for all the artery models.

Figure 7: Regardless of the plaque type, Nitinol stent oversizing resulted in a linear increase in both the arterial circumferential stresses (95th percentile) (left) and the lumen gain (right). For each oversizing ratio, the highest circumferential stresses were found to be in the artery with heavily calcified plaque, while the lowest were in the artery with lightly calcified plaque. On the other hand, the highest lumen gain was reported to be in the artery with lightly calcified plaque, followed by the arteries with heavily and moderately calcified plaques. In comparison, oversizing in a non-calcified artery resulted in a non-linear increase in arterial stresses, as well as in the lumen gain. Furthermore, diseased arteries were found to be less sensitive to oversizing than healthy arteries due to a smaller increase in the arterial stresses between each oversizing ratio.

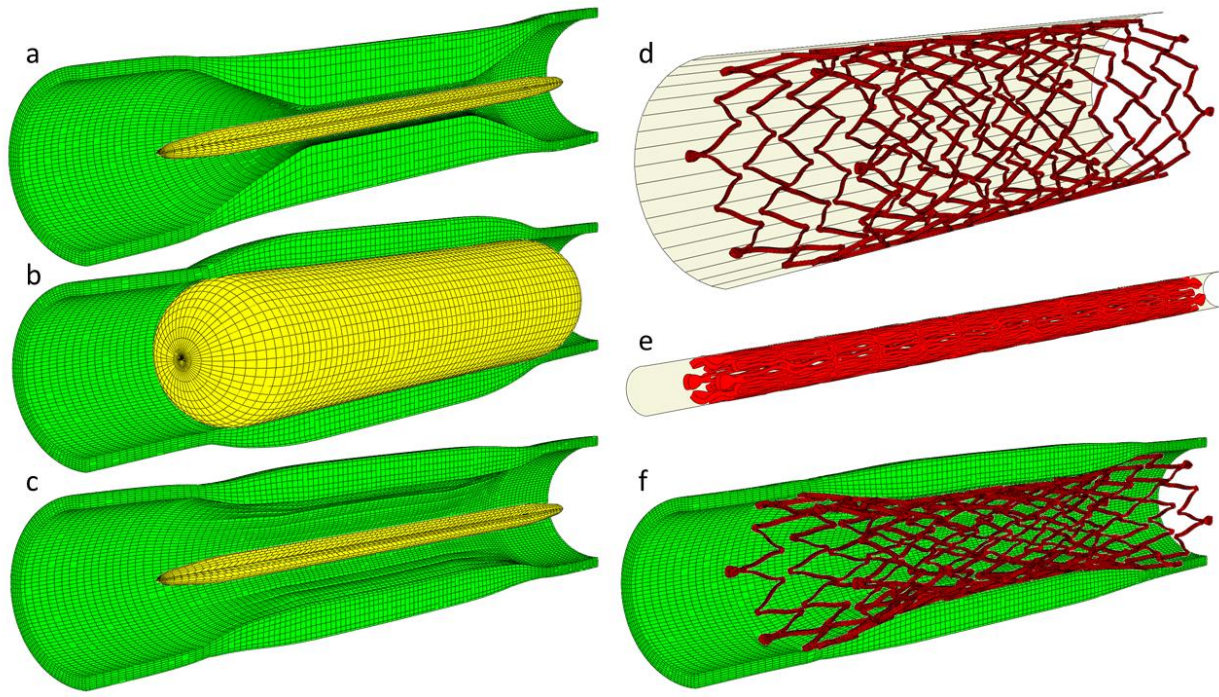


Figure 1. Gökgöl, Can

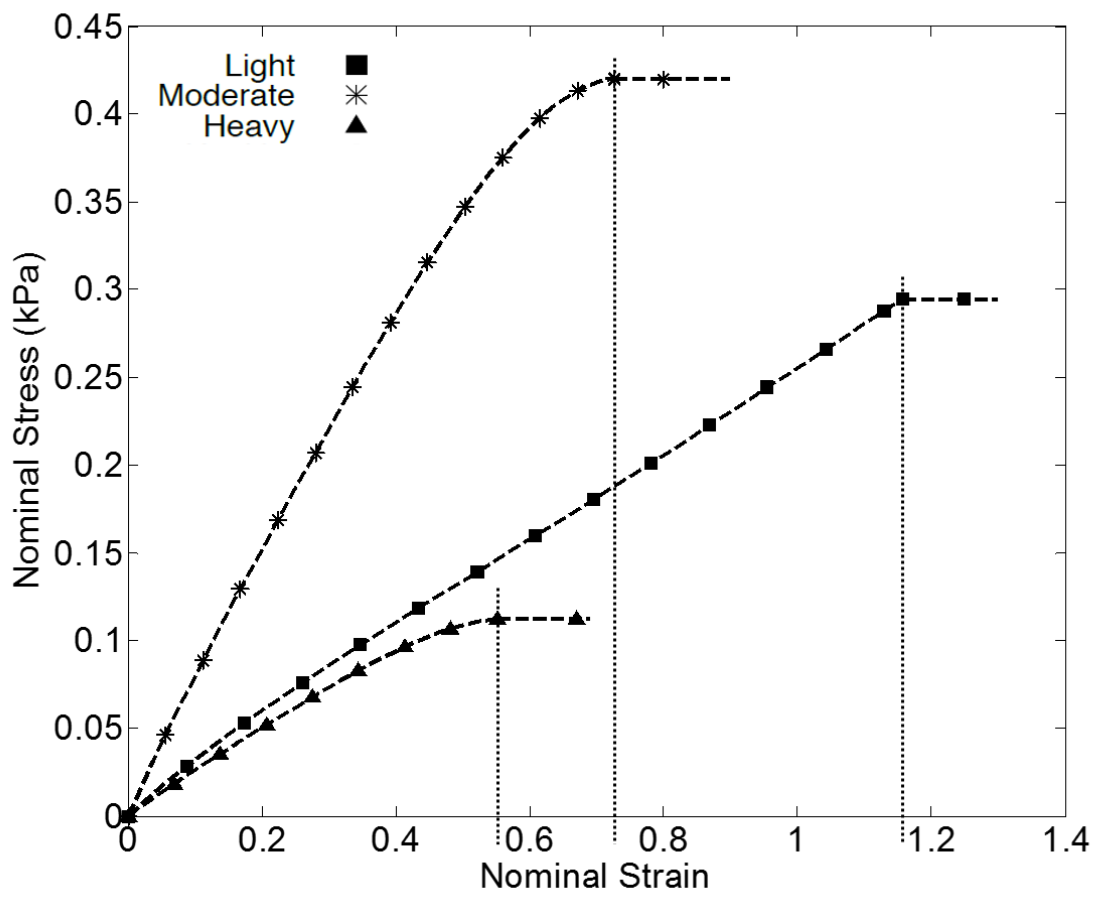


Figure 2. Gökgöl, Can

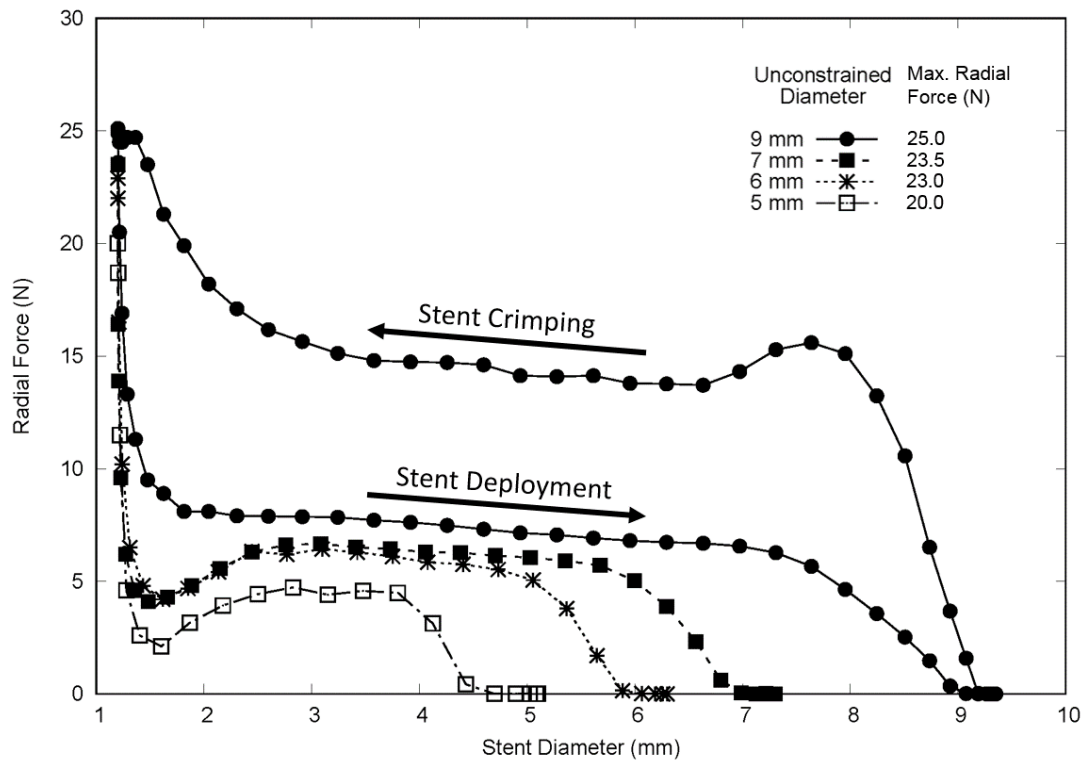


Figure 3. Gököl, Can

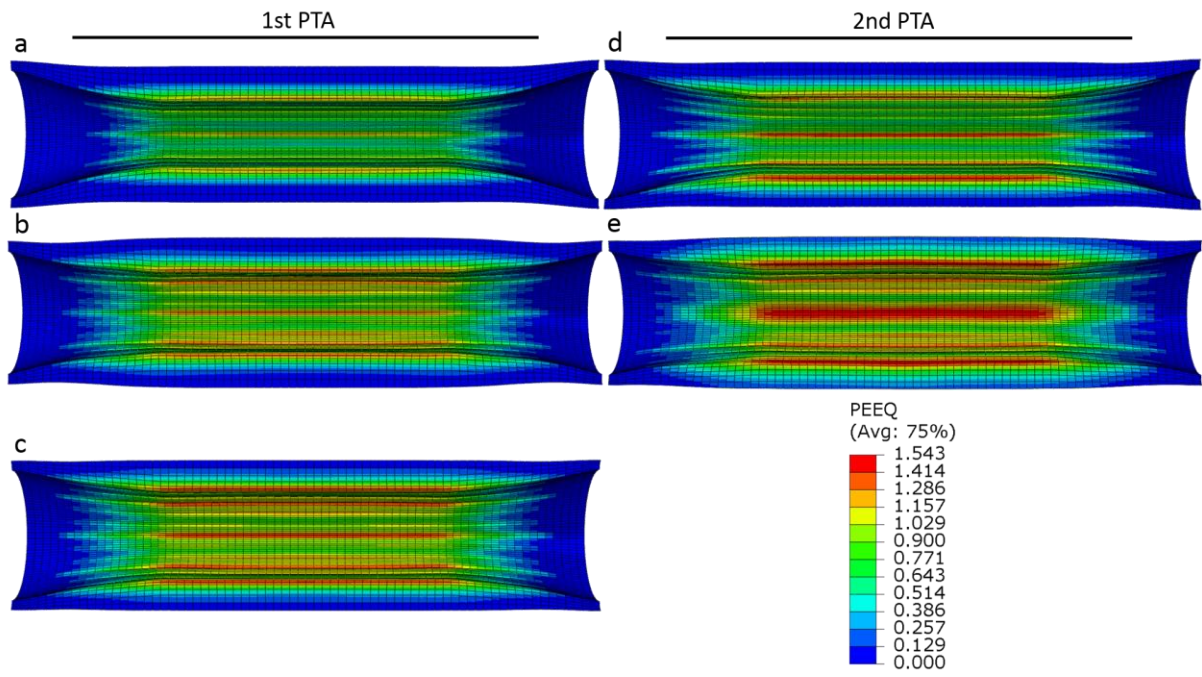


Figure 4. Gökgöl, Can

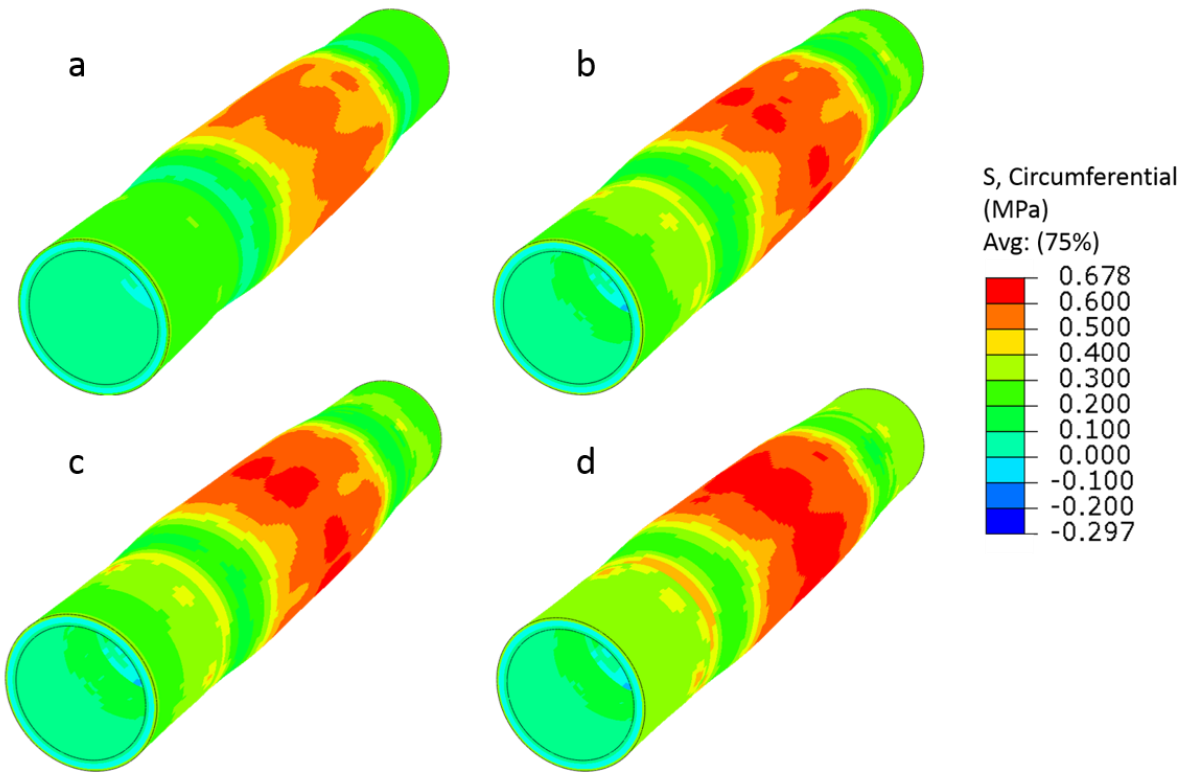


Figure 5. Gökgöl, Can

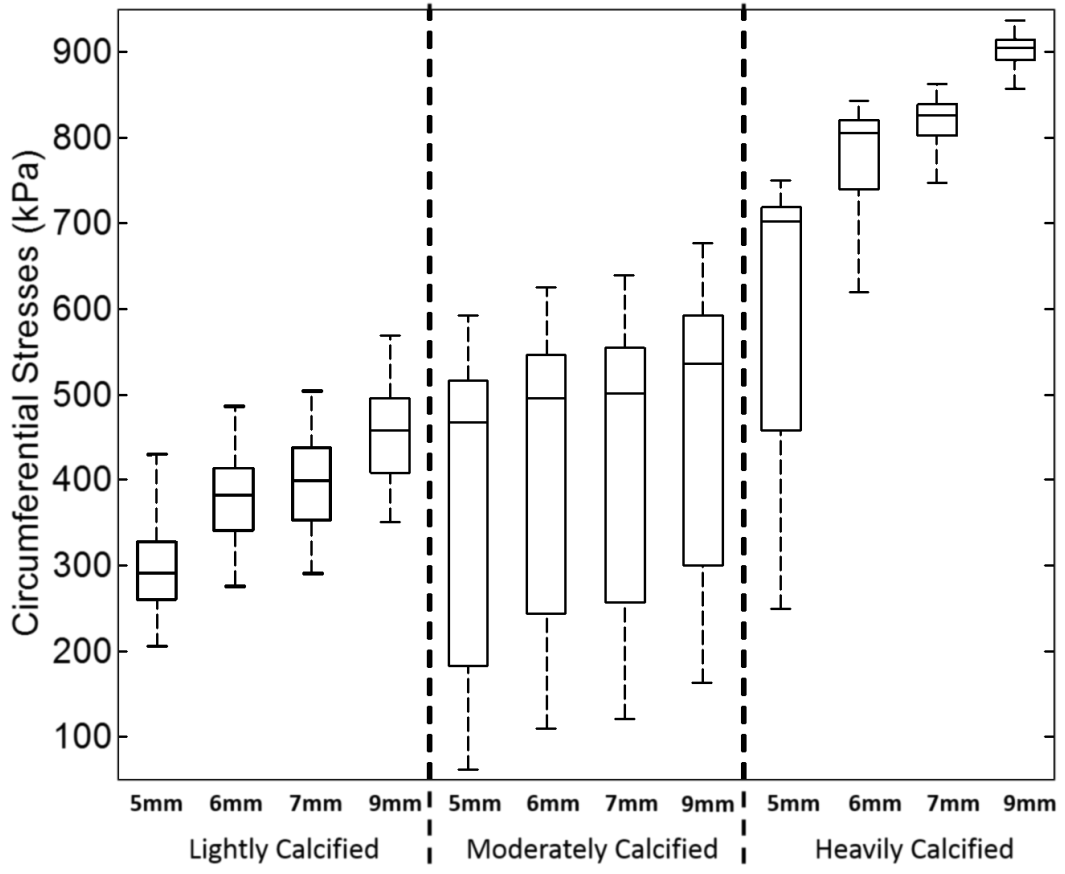


Figure 6. Gökgöl, Can

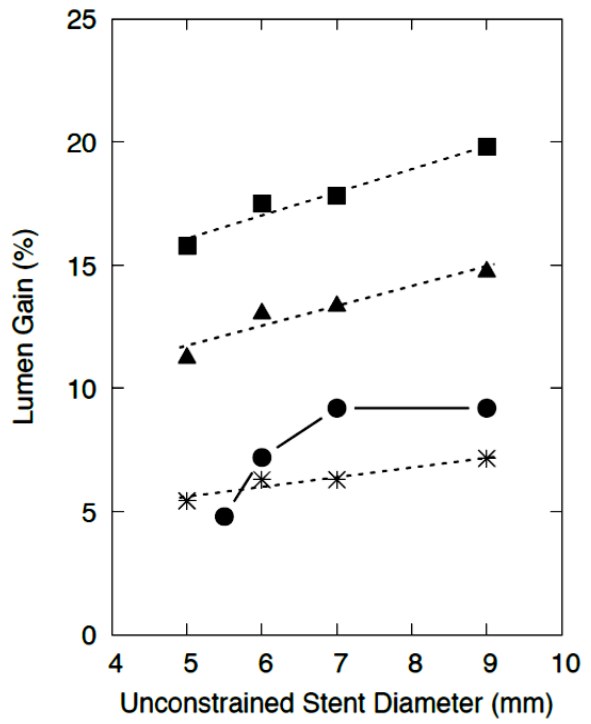
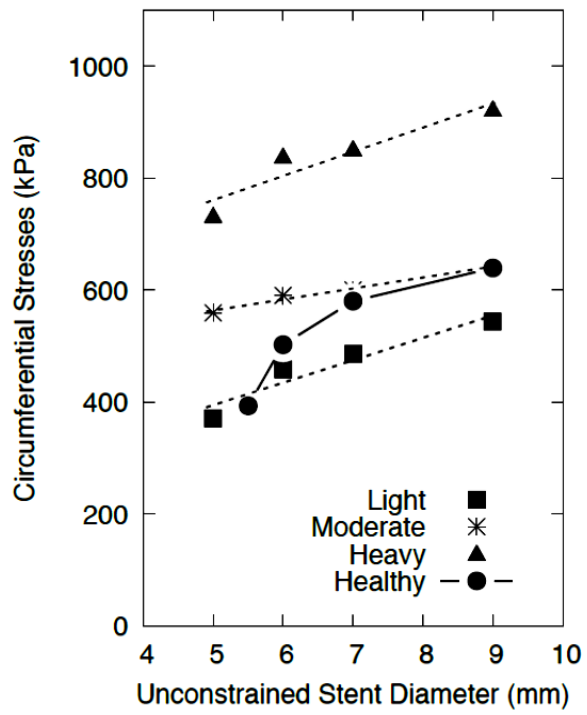


Figure 7. Gökgöl, Can